Supplementary Materials

Magnetite plaquettes are naturally asymmetric materials in meteorites

Queenie H. S. Chan[1], Michael E. Zolensky[1], James E. Martinez[2], Akira Tsuchiyama[3], and Akira Miyake[3]
[1]NASA Johnson Space Center, Houston, Texas 77058, USA.
[2]Jacobs Engineering, Houston, Texas 77058, USA.
[3]Graduate School of Science, Kyoto University, Kitashirakawa Oiwake-cho, Sakyo-ku, Kyoto 606-8502, Japan.

Contents

Supplementary Text

Interpretation of the EBSD data

The aspect ratio of the BSE images obtained by the JEOL FE-SEM is different from the EBSD data (e.g., portrait yellow box in Supplementary **Figure S7A** outlines the landscape image boundary of **Figure S7B**), because we have deselected the additional tilt correction option in the software in order to best match our BSE images to the EBSD maps. Individual discs are clearly discernable in the BSE image so we are able to distinguish the crystal boundaries with reference to the BSE and Argus forescattered electron (FSE) images.

The selected area for EBSD analysis includes surfaces of individual magnetite discs and cross-sections of stacks of magnetite plaquettes (**Figure 4A**). EBSD inverse pole figure (IPF) colored maps are shown in **Figure 4B**, Supplementary **Figures S7B** and **S8B**. IPF components use the RGB coloring scheme to indicate crystal orientations. Grains with their [001], [101] or [111] axes parallel to the sample projection direction of the IPF map (IPFX, normal to the rolling direction) are represented by red (R), green (G) and blue (B) color respectively. Intermediate orientations are indicated by mixing the RGB components accordingly. All colored data represent areas where the observed EBSD pattern could be well indexed by the calculated pattern of magnetite. The EBSD hit rate (degree of success in obtaining usable EBSD patterns) for magnetite was reduced to 40.8% due to the presence of a large volume of interstitial dolomite between magnetite plaquettes. Other than IPF maps, we have also studied the crystal misorientation profiles along lines defined on the plaquette surface and magnetite stacks. The lines are marked on the IPF maps, and the corresponding misorientation angles are presented as graphs in Figures (**Figure 4C-D**, Supplementary **Figures S7C** and **S7C**). It is worth mentioning that although an IPF map is not subject to the problem of the "wraparound" color effect, which isa common problem for All-Euler displays as a result of its coloring scheme. As the Euler angles approach to a limit, the R, G, or B components wobble between maximum and minimum value, which cause a significant color change for only a small variation in orientation and result in undesirable noise. Therefore, with the problem of the "wraparound" color effect, the misorientation only shows orientation change in projection parallel to a crystallographic axis, and thus it is not sensitive to changes in rotation about that axis. For instance, as seen in **Figures S9**, asterisks indicate locations with notable misorientation relative to the previous point (bottom graph), which is not shown in the profile of misorientation relative to the first reference point (upper graph). Magnetite has high crystal symmetry as it a member of the cubic inverse spinel space group. Under this geometry, the maximum observed θ is 45°, because any greater rotation is equivalent to a smaller rotation in the opposite direction. Thus, θ is conventionally represented by the minimum angle (i.e. disorientation) [1]. The observed θ spans the range from 0-45° but preferentially occurs <10° and >40°. The plaquettes are comprised of discs with a consistent rotation direction.

As we could observe changes in crystal orientation along the magnetite stack, we were also able to reconstruct the rotation orientation by observing the misorientation direction relative to the adjacent discs. However, we cannot obtain this information from examining the misorientation profile (relative to the last point) alone, because the misorientation angle only describe the amount of rotation about the common axis between the reference points, and thus it does not provide information about the direction component. The misorientation profile relative to the

first point gives more information regarding the direction component, however the software computed profile sometimes gives misinterpretation due to the symmetry of the cubic structure of magnetite. In order to investigate the rotation direction, we have also studied the extrapolated crystal orientation figure of each magnetite disc (similar to the **Figure 3D**), and marked the rotation directions on the misorientation profiles (**Figure 4D**).

Chiral asymmetry observed in meteorites

As extant life on Earth uses exclusively a single enantiomeric form of amino acids, sources of chiral asymmetry and its linkage to the origin of life on our planet have been extensively reviewed in the past decades. To date, it is still hotly debated whether extraterrestrial objects have played a dominant role in "seeding" the early Earth with abiotic organic compounds that reacted to form prebiotic molecules. Lee in proteinogenic amino acids likely indicates terrestrial contamination. Therefore, evaluations of the origin of homochirality often concentrate on non-proteinogenic amino acids, such as isovaline, which not only has rare terrestrial occurrence, but is also stereochemically stable and thus the enantiomeric ratio is less influenced by racemization. Several of the CCs were previously shown to present an ee for isovaline, including Orgueil (Lee = 15.2%)2, Murchison (Lee = 18.5%), GRA 95229 (Lee = 3%)3, and GRO 95577 (Lee = 11.0%)4. Lee data were not available for other meteorites covered in this study either because they have not been analyzed for amino acids, or because they contain a low amino acid abundance and thus the determination of individual amino acid enantiomeric ratio was impracticable.

List of abbreviations

ARES	Astromaterials Research and Exploration Science
BSE	Backscattered electron
CC	Carbonaceous chondrite
CH	Allan Hills 85085-like
CI	Ivuna-like
CK	Karoonda-like
CM	Mighei-like
CO	Ornans-like
CR	Renazzo-like
CV	Vigarano-like
E	Enstatite
EBSD	Electron backscatter diffraction
EDS	Energy-dispersive spectrometry
ee	Enantiomeric excess
FE	Field Emission
Fe_3O_4	Magnetite
JSC	Johnson Space Center
LABE	Low-angle backscattered electron detector
NASA	National Aeronautics and Space Administration
NSS	NORAN System Seven
SEM	Scanning electron microscopy

Supplementary Figures and Legends

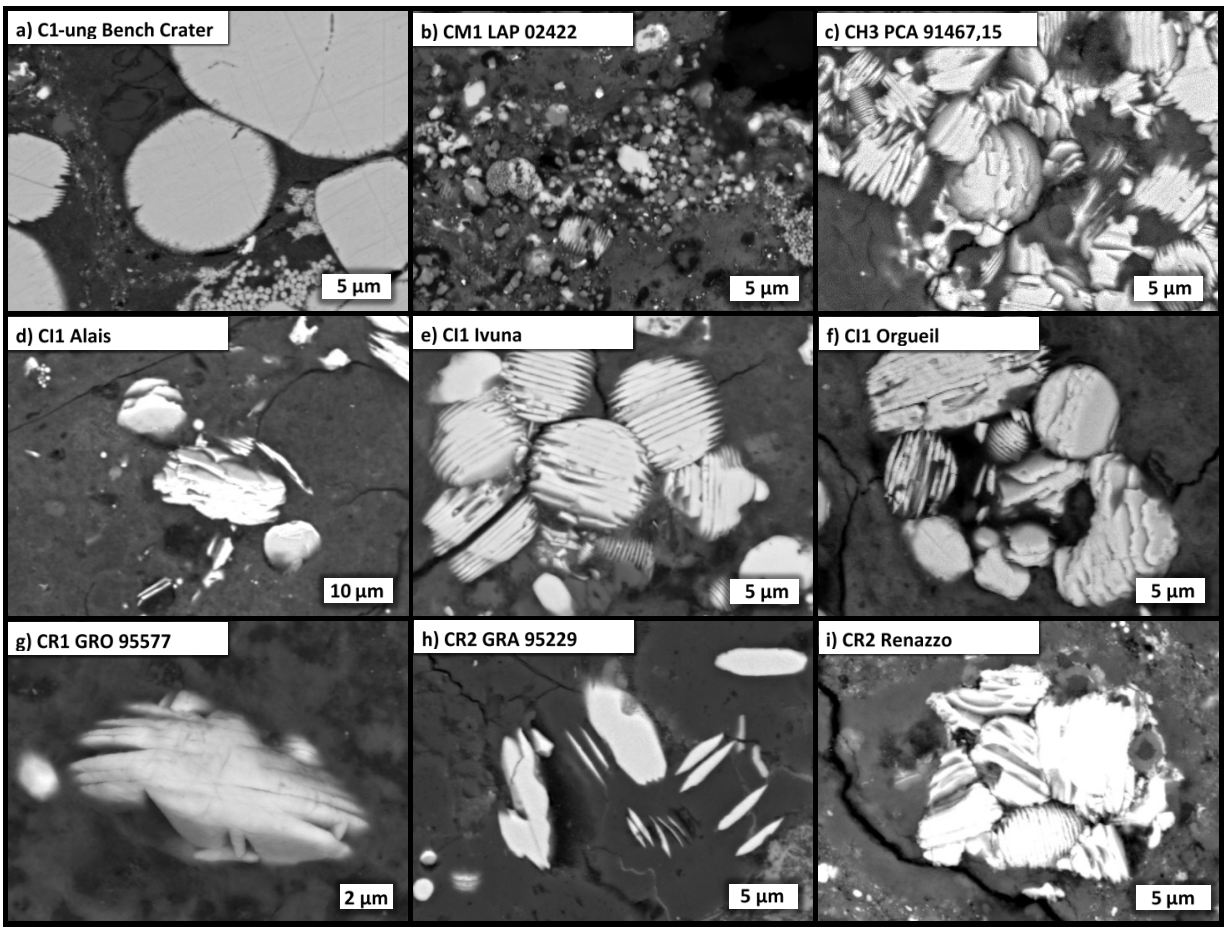

Figure S1
BSE images of the magnetite plaquettes observed in the nine CCs in this study. We took measurements of the geometry of the free-standing magnetite plaquettes (Supplementary **Figure S3** and **Table 1**). The diameter of the largest disc (in the middle of the stack) ranges from 5.7 to 15.6 µm. The thickness of the individual discs ranges from 0.2 to 0.6 µm, while the disc spacing was 0.1 to 0.4 µm. The number of discs in a stack varies from 4 to 24, and the thickness of the plaquettes is generally smaller for stacks that comprise a larger number of discs. The measurements generally agree with the data reported for Orgueil by Hua and Buseck[5].

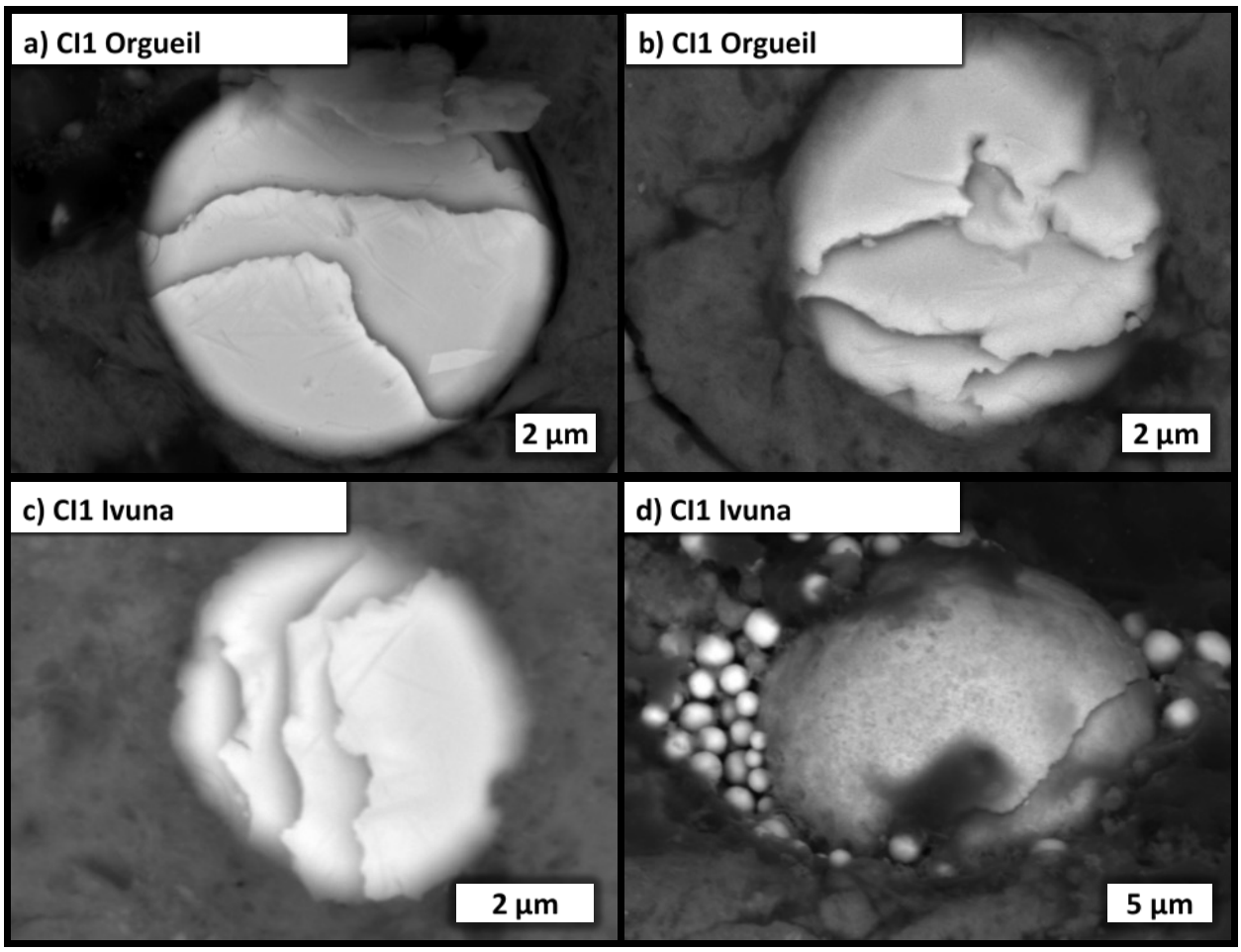

Figure S2
BSE images of the "cabbage-like" morphology of magnetite. Other than isolated spherules, framboids and stacked plaquettes, we have also observed a “cabbage-like” morphology that has not been previously described for the CC magnetite.

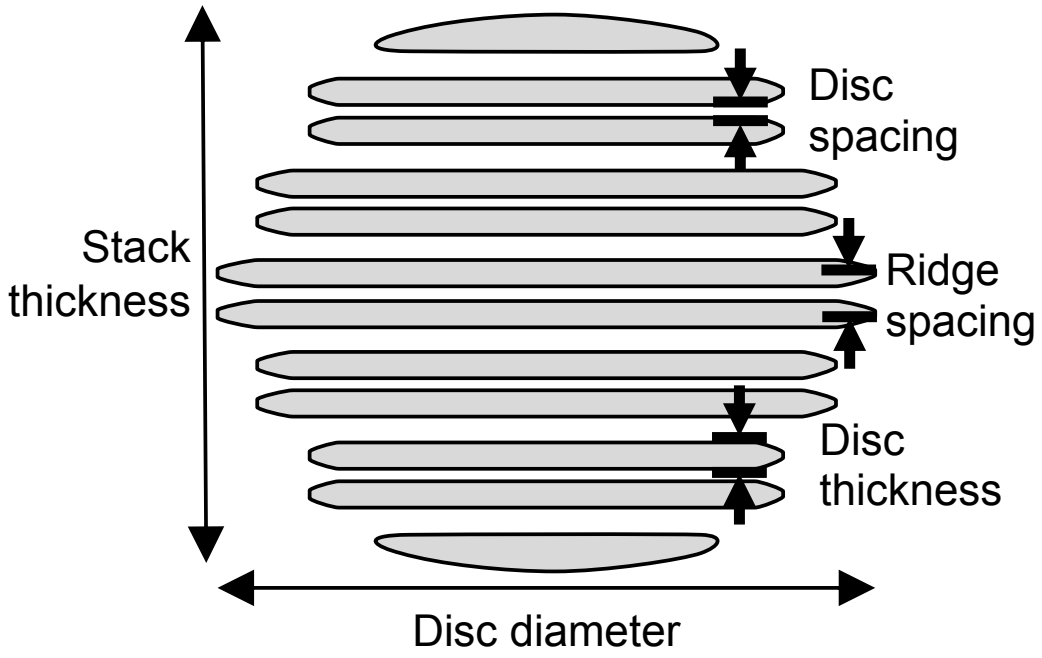

Figure S3
A schematic diagram of the geometry measurements of a well-formed magnetite plaquette.

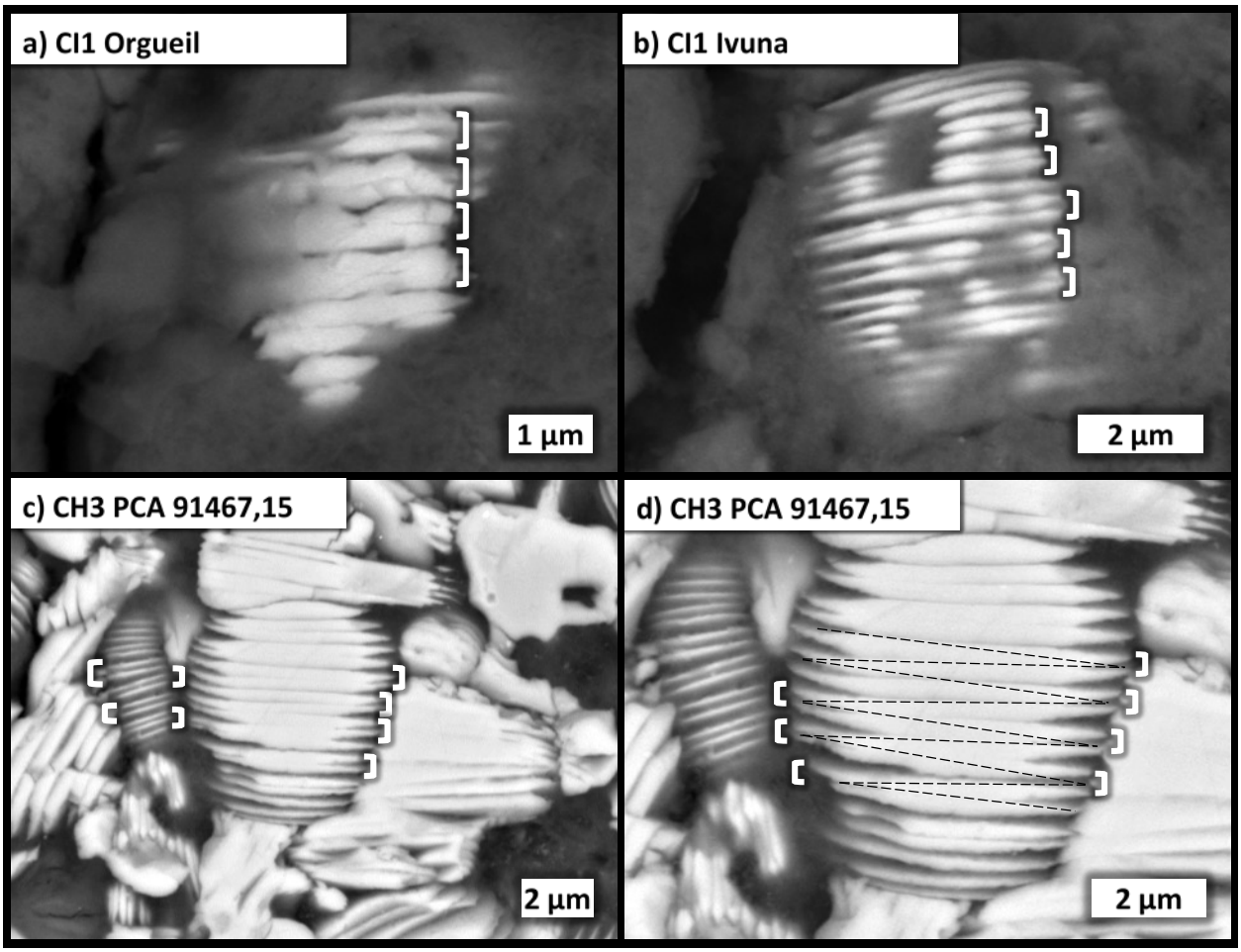

Figure S4
Magnetite plate-doublets marked by brackets. (**a**) – (**c**) show similar feature found in different meteorites. (**d**) is an enlarged image of (**c**) that shows an apparent zigzag pattern of the magnetite disc arrangement.

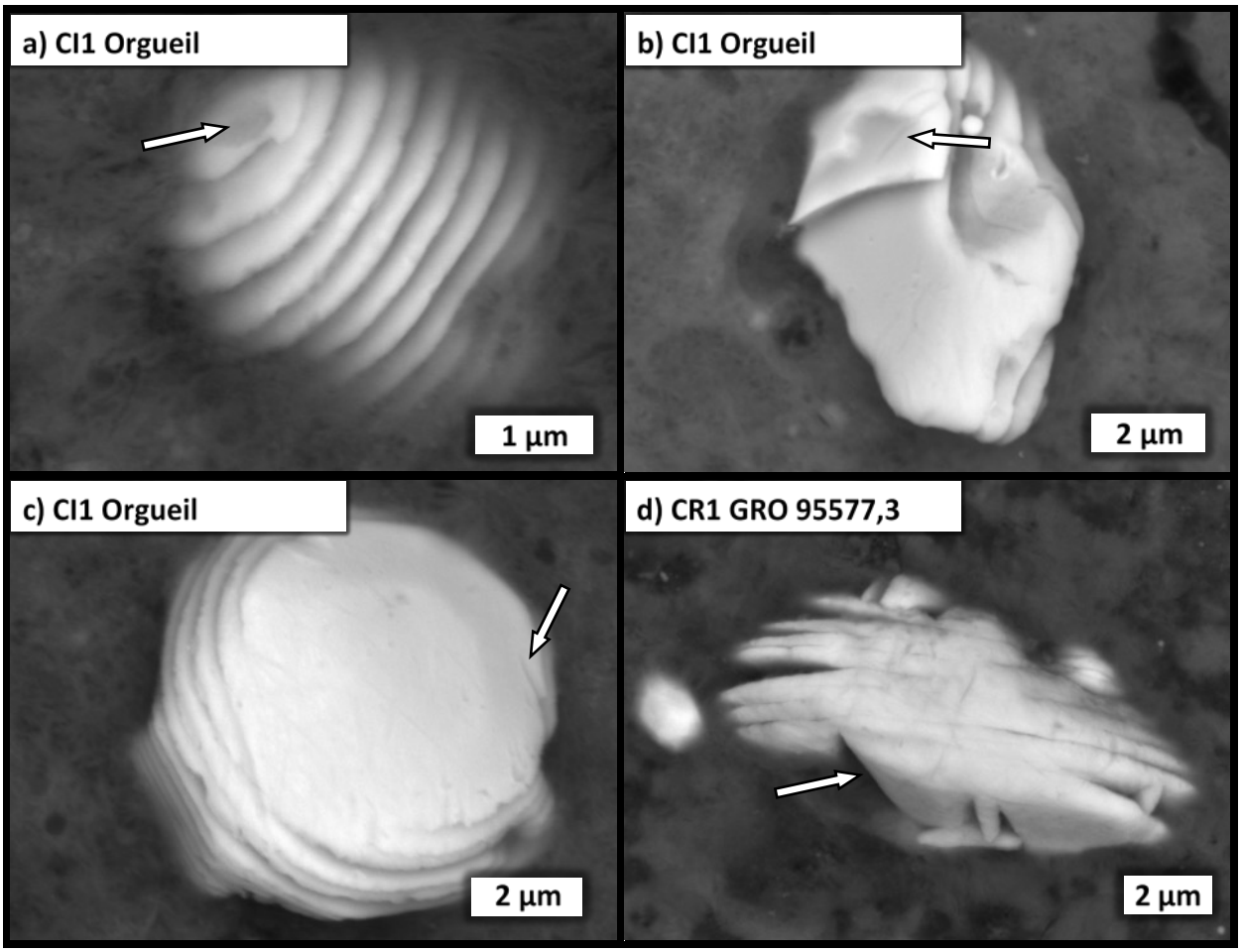

Figure S5
Spiral-like features of magnetite plaquettes. (**a-b**) The arrows mark the apparent hollow cores and the spiral features around it; (**c**) The arrow marks an indentation on the plate that resembles a screw dislocation slip feature; (**d**) The arrow marks an apparent indentation. However, these features are not prominent and their associations with screw dislocation feature is weak.

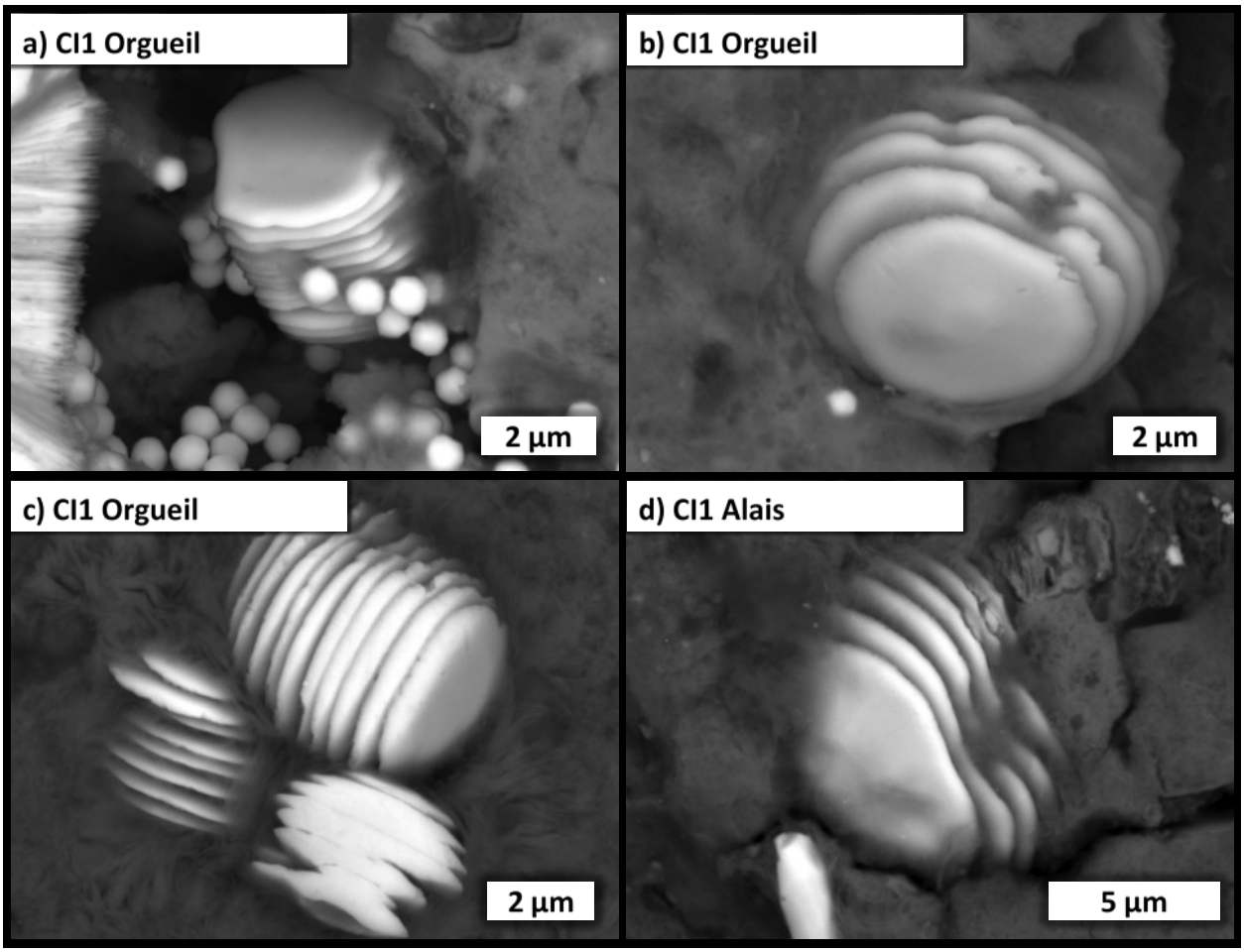

Figure S6
Non-spiral like features of magnetite plaquettes.

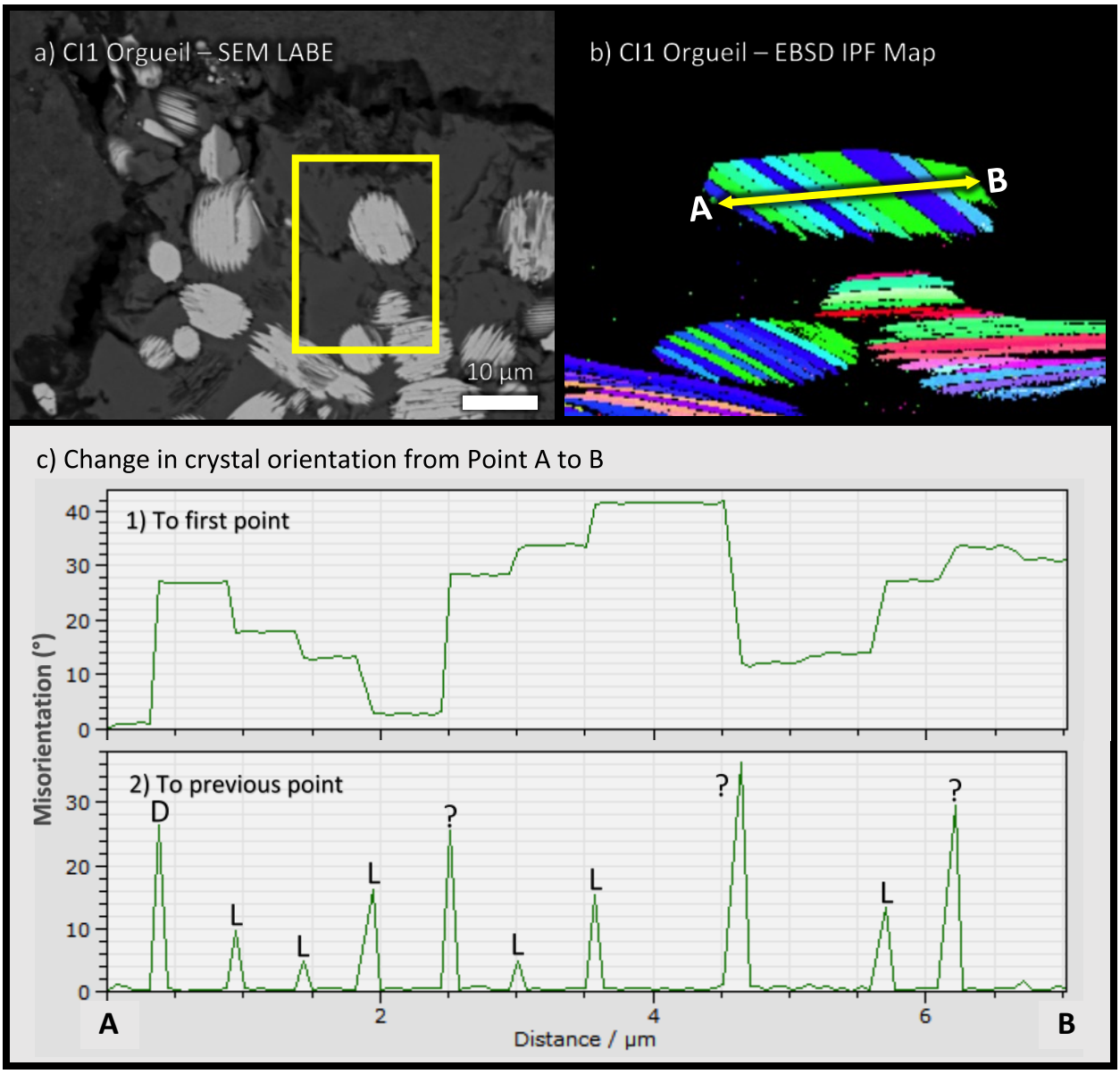

Figure S7
EBSD data for a magnetite stack (Stack 1) in Orgueil. (**a**) BSE image; (**b**) IPFX map, change in crystal orientation has been obtained for Line A-B; (**c**) Graphs showing the change in crystal orientation relative to (1) the first point (i.e. Point A) and (2) the previous point on Line A-B. Rotation directions are indicated with (D) & (L) for clockwise & counterclockwise rotation respectively. (?) denotes abrupt changes in crystal orientation of which the directions do not conform to the arbitrary rotational axis.

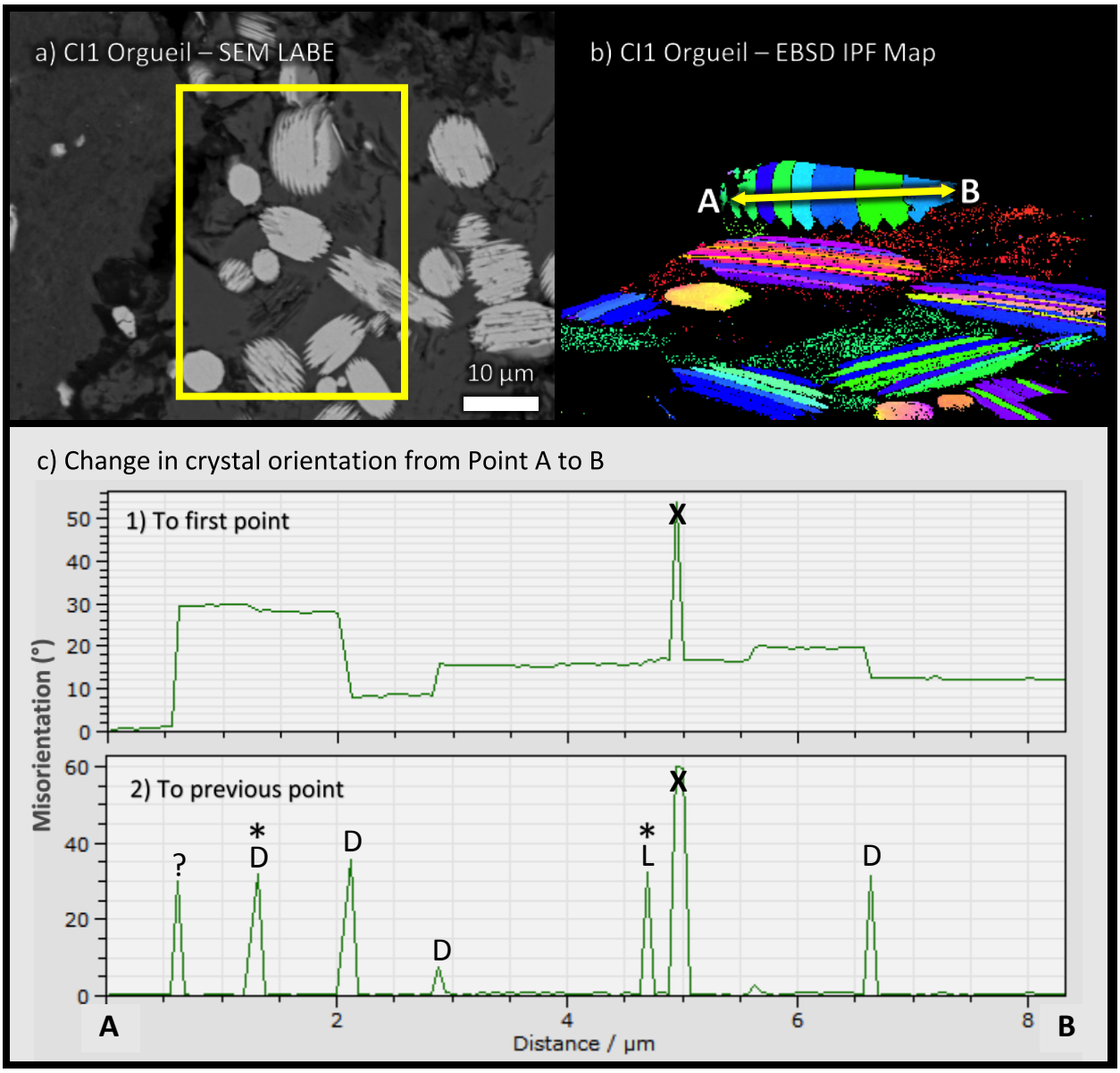

Figure S8
EBSD data for a magnetite stack (Stack 2) in Orgueil. (a) BSE image; (b) IPFX map, change in crystal orientation has been obtained for Line A-B; (c) Graphs showing the change in crystal orientation relative to (1) the first point (i.e. Point A) and (2) the previous point on Line A-B. *denotes locations where changes in crystal orientation was observed in graph (2) and not in graph (1). Rotation directions are indicated as in **Figure 4**. (X) marks a peak incorrectly displayed in the graph generated by the analytical software, no change in crystal orientation was observed for that point. (?) denotes abrupt change in crystal orientation of which the direction does not conform to the arbitrary rotational axis.

Supplementary References

1 Wheeler, J., Prior, D., Jiang, Z., Spiess, R. & Trimby, P. The petrological significance of misorientations between grains. *Contributions to Mineralogy and Petrology* **141**, 109-124, doi:10.1007/s004100000225 (2001).

2 Glavin, D. P. & Dworkin, J. P. Enrichment of the amino acid L-isovaline by aqueous alteration on CI and CM meteorite parent bodies. *PNAS* **106**, 5487-5492 (2009).

3 Pizzarello, S., Huang, Y. & Alexandre, M. R. Molecular asymmetry in extraterrestrial chemistry: Insights from a pristine meteorite. *PNAS* **105**, 3700-3704 (2008).

4 Glavin, D. P., Callahan, M. P., Dworkin, J. P. & Elsila, J. E. The effects of parent body processes on amino acids in carbonaceous chondrites. *Meteoritics & Planetary Science* **45**, 1948-1972 (2011).

5 Hua, X. & Buseck, P. R. Unusual forms of magnetite in the Orgueil carbonaceous chondrite. *Meteoritics & Planetary Science* **33**, A215-A220, doi:10.1111/j.1945-5100.1998.tb01335.x (1998).